Impact of temperature increments on tunneling barrier height and effective electron mass for plasma nitrided thin SiO_2 layer on a large wafer area

G. Aygun,[1,2,a)] G. Roeder,[1] T. Erlbacher,[1] M. Wolf,[1] M. Schellenberger,[1] and L. Pfitzner[1]
[1]*Fraunhofer IISB, Schottkystrasse 10, 91058 Erlangen, Germany*
[2]*Department of Physics, Izmir Institute of Technology, TR-35430 Urla, Izmir, Turkey*

(Received 10 May 2010; accepted 21 July 2010; published online 13 October 2010)

Thermally grown SiO_2 layers were treated by a plasma nitridation process realized in a vertical furnace. The combination of a pulsed-low frequency plasma and a microwave remote plasma with $N_2/NH_3/He$ feed gas mixture was used to nitride the thermally grown SiO_2 gate dielectrics of MIS structures. Temperature dependency of effective masses and the barrier heights for electrons in pure thermally grown SiO_2 as well as plasma nitrided SiO_2 in high electric field by means of Fowler–Nordheim regime was determined. It is frequently seen from the literature that either effective electron mass or barrier height (generally effective electron mass) is assumed to be a constant and, as a result, the second parameter is calculated under the chosen assumption. However, in contrast to general attitude of previous studies, this work does not make any such assumptions for the calculation of neither of these two important parameters of an oxide at temperature ranges from 23 to 110 °C for SiO_2, and 23 to 130 °C for nitrided oxide. It is also shown here that both parameters are affected from the temperature changes; respectively, the barrier height decreases while the effective mass increases as a result of elevated temperature in both pure SiO_2 and plasma nitrided SiO_2. Therefore, one parameter could be miscalculated if the other parameter, i.e., effective mass of electron, was assumed to be a constant with respect to variable physical conditions like changing temperature. Additionally, the barrier heights were calculated just by taking constant effective masses for both types of oxides to be able to compare our results to common literature values.
 [doi:10.1063/1.3481348]

I. INTRODUCTION

In order to overcome the scaling limit of conventional SiO_2 gate dielectrics due to high tunneling currents and reliability concerns, different gate materials possessing a higher relative dielectric constant at comparable properties, i.e., less oxide charges, sharpness of interfacial region, oxide's strength to high *E*-fields, to those of thermal oxides can be applied. Hereby, lower leakage currents between gate and channel region can be achieved at a comparable equivalent oxide thickness (EOT) despite increasing the physical thickness. Either the high permittivity (high-*k*) materials, such as single metal oxides like TiO_2, Y_2O_3, Ta_2O_5, ZrO_2, HfO_2, and their silicates as well as ferroelectrics, are being investigated as alternative dielectrics,[1–4] or some further processing on thermally grown SiO_2 layer to improve its properties like plasma nitridation, ion implantation, further annealing steps in various gas environments has been done.[5] Important film properties as well as interfacial structure affecting especially electrical properties including dielectric constant and refractive index of the grown film, depend on the growth parameters as well as the initial thin film constitution.[6–8] Therefore, it should be noted that the applied physical conditions on thermally grown SiO_2 must be well controlled through the whole stages during further processing steps in order to improve its dielectric properties.

Having a very sharp interface on Si, thermally grown SiO_2 has excellent electrical and technological properties. Since it is the main perfect insulator of microelectronics technology, it was chosen here for the gate oxide to be modified. Green *et al.*[5] summarized literature as follows: even though plasma nitridation processing of thin films improves the insulating quality of the film, resulting in an increment in its dielectric constant due to nitrogen incorporation, it meanwhile creates some defects inside the oxide bulk as well as at the interfacial region. Therefore, conduction mechanisms of plasma nitrided SiO_2 layer should be determined with respect to different applied physical conditions.

Nitrided SiO_2, i.e., SiO_xN_y (SiON), on the other hand, is an important material since it is appropriate for optoelectronic devices such as waveguides, and has become a standard in optoelectronics industry.[9] It can also be used for photovoltaic industry especially for antireflection multilayers in combination with hydrogenated silicon nitride. Additionally, the passivation effect of SiON is very promising for solar cell rear surface, which is a high constraint on thin solar cells. Moreover, thin SiON layers are of interest and used in high-*k* dielectric complementary metal oxide semiconductor (CMOS) technology. Therefore, exploring the leakage current characteristics of SiON as well as those of SiO_2 is an important achievement for CMOS technology as well as for obtaining efficient solar cells.

In this work, we examined the properties of oxide and nitrided oxide under the applied high *E*-field conditions. We

a)Electronic mail: gulnuraygun@iyte.edu.tr.

have determined the effective mass of tunneling electrons and the barrier heights in pure thermally grown SiO_2 as well as in plasma nitrided SiO_2 in high electric field regime for temperature ranges from 23 to 110 °C for SiO_2, and from 23 to 130 °C for nitrided oxide. The effective mass is generally assumed to be a constant and as a result, barrier height is calculated. However, in this work, we do not make any such assumptions for the calculation of neither of these two important parameters of an oxide at temperatures ranging from 23 to 110 °C for SiO_2 and to 130 °C for nitrided oxide. We will show that both parameters are affected by temperature changes; the barrier height decreases with temperature increments while the effective mass increases in both pure SiO_2 and plasma nitrided SiO_2. Additionally, we calculated the barrier heights as if effective mass of tunneling electrons were constant at room temperature (RT) value to be able to compare our results to this common attitude's results. It was shown that barrier heights change only in a very small range when the effective mass of tunneling electrons is assumed to be constant.

II. LITERATURE REVIEW

Even though the leakage current through ideal insulators is assumed to be extremely small, however, in real structures, charges leak through the oxide layer of metal insulator semiconductor (MIS) system to some degree. Depending on the applied physical conditions on MIS capacitors, a few models for leakage current mechanisms have been developed to define the effective working condition regimes of MIS structures like SiO_xN_y and SiO_2 reference dielectrics. Some of these conduction mechanisms are categorized as (i) electronic hopping conduction, (ii) field assisted emission, (iii) Poole–Frenkel effect, (iv) double barrier tunneling, (v) direct tunneling (DT), (vi) Fowler–Nordheim (FN) tunneling, and (vii) Schottky emission.[10]

It is well known that when an external E field is applied onto a crystal structure, charge carriers do not only feel the effect of this external electric field but also the internal effects originating from the atomic cores and other carriers. Therefore, charge carriers do not move inside the crystal system as if they are free charges. Effective mass is, therefore, defined in periodic crystal structure and model the periodic atomic potential.[11] Nevertheless, the above explanation loses its meaning for ultrathin amorphous dielectric layers as a result of lack of crystal periodicity. Moreover, Mao and Wang[12] referred in their work to another study in which it was declared that amorphous silicon dioxide is believed to have similar band structure properties to those of alpha quartz and the same technique can be applied to the more disordered structure of SiO_2.[13]

Many studies have been devoted to electron tunneling through the oxide layer under high applied electric field regimes, i.e., FN tunneling.[14] In FN regime, electrons actually partly tunnel through the band gap and partly propagate in the dielectric's conduction band. For electron tunneling, the effective mass of electrons in the SiO_2 oxide conduction band, m^*, is generally assumed to be a constant between $0.3m_e$ and $0.5m_e$ where m_e is the free electron mass, and accordingly, the tunneling barrier is calculated. However, it is seen from literature that there exist some discrepancies when one of these values is assumed to be a constant and, accordingly, the other parameter is calculated.[15,16] In fact, neither of these parameters is constant and may change under the applied conditions as well as constituting material formation inside the oxide structure from SiO_2 to nitrided SiO_2, i.e., SiO_xN_y.

Fukuda *et al.*[17] analyzed the tunnel current through ultrathin (1.27–8.12 nm thick) gate oxides by proposing two effective masses for such an electron, i.e., a tunneling effective mass for DT part and conduction effective mass for propagating in the conduction band. They explained the direct current, quantitatively, through ultrathin gate oxides by multiple-scattering theory (MST). In MST, SiO_2 layer was segmented into multiple rectangular potential barriers in which conduction barrier height was used as 3.34 eV at the $SiO_2/Si(100)$ interface and DT effective mass of $0.35m_0$. The FN tunnel current oscillation was reproduced applying the oxide conduction band effective mass of $m^*_{ox}=0.60m_0$. They evaluated the direct tunnel electron mass as a fitting parameter when compared the measured current to MST current in the oxide thickness ranging from 3 to 5 nm.

Nadimi *et al.*[18] studied MOSFETs with lightly doped silicon oxynitride (SiO_xN_y) gates and formulized m^*/m_e. They interpreted a strong dependence of the effective electron mass depending on the oxide thickness and atomic nitrogen concentration, and showed that the electron effective mass was found to increase as both layer thickness and nitrogen concentration decreases.

Ng *et al.*[15] studied the influence of nitrogen on tunneling barrier heights and effective masses of electrons and holes at lightly nitrided layers having a nitrogen content changing from 1.8 to 4.5 at. % on SiO_2/Si interface, as well as pure SiO_2. They concluded that barrier height decreases while effective mass increases with respect to an increased level of nitridation from 1.8 to 4.5 at. % nitrided SiO_2 films. They gave a summary that effective mass and barrier height changed from $0.36m_e$ to $0.5m_e$, and from 2.9 eV to 3.15 eV, respectively.

Städele *et al.*[19] provided not only theoretical but also experimental arguments that the effective mass used as a fitting parameter in their calculations of tunneling currents through thin (<4 nm) SiO_2 layers increased drastically even above $1.5m_e$ as oxide thickness was reduced.

Mao and Wang[12] studied tunneling currents through lightly nitrided silicon dioxide and oxide stacks. They tabulated the effect of nitrogen concentration of the oxide layer on the effective mass of electrons. According to their results, nitrogen of 2.8%, 5.7%, 8.7%, 11.8% resulted in 0.73, 0.93, 2.3, $3.8m_e$ for effective masses, respectively. They concluded that the average effective electron mass at the bottom of the conduction band will increase with increased nitrogen concentration. They stated that a larger effective electron mass resulting in smaller DT and FN tunneling currents is well known. Therefore, they concluded that the tunneling current would be reduced if the other factors that could affect tunneling remain constant and/or change only slightly.

Horiguchi and Yoshino[20] evaluated interfacial potential

barrier heights and effective electron masses for ultrathin silicon oxides (1.5–4.4 nm) on Si. They assumed thick oxides when thicker than 3.6 nm and performed their calculations with a constant m^* value. They assumed thin oxides when they are thinner than 3.1 nm with variable m^*. Potential barrier heights of 1.3 eV, 1.6 eV, 1.8 eV and effective electron masses of $3.0m_e$, $1.3m_e$, $1.0m_e$ were obtained for 1.5 nm, 2.4 nm, and 3.1 nm thick oxides, respectively.

Furthermore, Mao *et al.*[21] studied the band structure of lightly nitrided silicon oxide on the basis of the first principle calculations. They have shown that there are defect like states in the band gap and maybe originated from the vacancies substituting the oxygen atoms. They declared that effective electron mass increases with respect to lightly nitridation of oxides in terms of FN regime. According to increasing effective mass as a result of light nitridation, leakage current with definitions of FN regime should be decreased and even lower than that of SiO_2 layer. They concluded that this is, however, not the case in reality when leakage current levels are compared to experimental results. Since they showed with their method that there are defect like states in the band gap, so defect assisted tunneling should be taken care of additional to FN tunneling current. Their conclusion is that since defect assisted tunneling may make a larger contribution to the gate leakage current due to defect like energy levels within the energy band gap, a single leakage mechanism is not enough to interpret the experimental leakage current.

Some additional research has been traced from literature about tunneling characteristics as a result of temperature changes. Hadjadj *et al.*[22] obtained barrier heights with respect to temperature changes just by taking a constant effective electron mass of $0.5m_e$ for samples whose thicknesses were changing between 3.5 and 12 nm, and they showed that barrier height was decreased when the temperature was increased.

Additionally, Costato *et al.*[23] summarized the combined effective mass of holes in silicon in the temperature range of 40–400 K. They used the energy band analysis to explain that approximation of a constant effective mass seems to be inadequate to describe the transport properties of holes in Si above 40 K. They showed that the effective mass of holes increases significantly from 40 to 400 K due to nonparabolic character of the second energy band E_2. It was explained that when the heating is realized then the carriers can populate deeper regions in the band E_2, and therefore the nonparabolic nature of E_2 away from $k=0$ becomes significant showing an increase in the effective mass of E_2 toward the value of effective mass of E_1. Increased temperature's effect on effective mass of holes for the energy levels of E_1, E_2, and E_3 was explained in details in this publication, and references therein.

Mao[24] remarks from his calculations that the temperature sensitivity of the tunneling current strongly depends on the effective electron mass. Horiguchi and Yoshino[20] gave their results of barrier height and effective electron mass with respect to oxide thickness showing that Φ_B decreases and m^* increases when the oxide thickness gets smaller. They have especially obtained barrier height of 1.3 eV and effective electron masses of $3m_e$ for 1.5 nm thick oxide.

From the results given above as literature review, it is clear that there are some discrepancies among different research groups. For example, Nadimi *et al.*[18] showed that effective mass decreases as nitrogen concentration increases, on the other side Ng *et al.*[15] and Mao and Wang[12] showed the opposite behavior. Nadimi *et al.* used a self-consistent model including quantum mechanical effects for ultrathin oxides, while Ng *et al.* used an analytical expression, and Mao *et al.* extracted the effective mass by evaluating the curvature of band structure at the minimum of the conduction band, all using DT regime. The reason could be the different methods, models, or even different regimes, i.e., DT or FN, used for determination of effective electron mass.

Even at RT conditions, only few studies come across in the literature that both parameters were calculated at the same time without making any assumptions.[15] To the knowledge of the authors, no such studies for the calculation of both parameters at the same time in the range of an increased temperature regime without making any assumptions has been done. Another important outcome of this article is that effective mass is not constant as many authors claim. Therefore, this work contains important analytical results of both barrier height and effective mass values for temperatures ranging from 23 to 110 °C for a thermally grown 5 nm thick SiO_2 used as a reference film, and from 23 to 130 °C for a nitrided oxide film.

III. EXPERIMENTAL PROCEDURE

This section contains two main parts: (i) nitridation process of thermally grown 5 nm thick SiO_2 layers and (ii) electrical measurements. *p*-type Si wafers with a resistivity of 4–6 Ω cm and a diameter of 150 mm were used as substrates. Polygated MIS test structures were fabricated by applying a local oxidation of silicon (LOCOS) process to investigate capacitance-voltage (*C-V*) and current-voltage (*I-V*) properties of plasma nitrided oxides versus thermally grown oxide layers. After growth of a 625 nm thick field oxide, the MIS structures were defined by etching. On the etched and cleaned Si, a 5 nm gate oxide was grown by dry thermal oxidation. Then, one of these thermally grown 5 nm thick SiO_2 oxide films was processed in a vertical furnace having the combination of a pulsed low frequency (LF) and a microwave (MW) remote plasma by using $N_2/NH_3/He$ feed gas mixture allowing a wide variation in nitridation conditions regarding to nitrogen incorporation, ion energies, plasma damage, and plasma homogeneity (Fig. 1). The parameter settings used for the nitridation process in these experiments are given in Table I. After the plasma-assisted nitridation in the furnace, poly-Si was deposited at 620 °C by low pressure chemical vapor deposition (LPCVD) and was *n*-doped under a 30 min $POCl_3$ processing at 950 °C. Poly-Si gated electrodes of the MIS test structures were obtained after lithographical processing, etching and cleaning steps of LOCOS process.

The leakage currents were measured with an HP 4145A Semiconductor Parameter Analyzer in dark conditions from

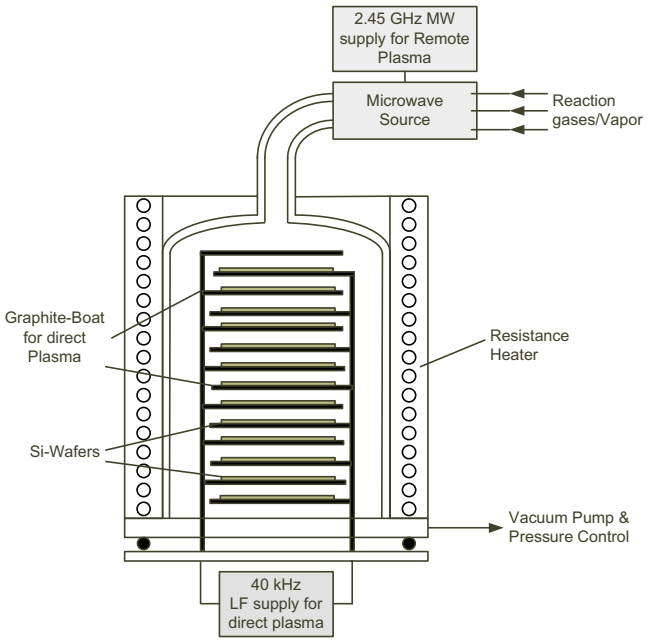

FIG. 1. (Color online) Schematic view of a vertical furnace used in nitridation process of thermally grown SiO_2 film.

MIS structures having 33.8×10^{-3} mm^2 gate area starting from RT (23 °C) to an elevated temperature of 110 °C for SiO_2 and 130 °C for nitrided oxide film. After the first measurement at RT, the device was heated to 30 °C and measured at this temperature again. It was, then, followed by another cycle of heating step to 50 °C temperature, the measurement was realized at this temperature, and it was followed by another cooling step down to RT. This process cycle, i.e., heating from RT to the required temperature, making the measurements at the heated device temperature and cooling down the device to RT, was continued until 110 °C for SiO_2 and 130 °C for nitrided oxide measurement with 20 °C increment in each step was realized.

Following electrical measurements at the required device temperatures, transmission electron microscopy (TEM) picture of nitrided oxide with high resolution TEM (HRTEM) using Philips CM 300 was taken (Fig. 2). It is clearly seen that there are two-layered oxide stack film combined from SiO_2 as the deeper layer and nitrided oxide on the surface.

Cho *et al.*,[25] in a recent study, chemically investigated their nitrided oxide films subjected to *postnitridation annealing, and showed that the unstable* N_2 molecule at the interface diffused out, while N on the surface is chemically bonded to Si_3 by changing its situation to a more stable form by synchrotron radiation x-ray photoemission spectroscopy and medium energy ion scattering spectroscopy techniques.

In our experiments, plasma-assisted nitridation was realized on thermally grown oxide films. As it was explained in the upper part of this section, poly-Si gated electrodes of

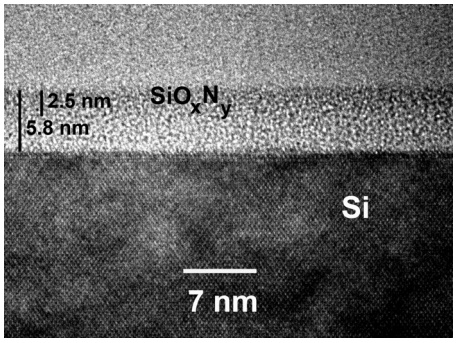

FIG. 2. HRTEM picture taken from nitrided oxide film.

MIS test structures were obtained after lithographical processing, etching and cleaning steps of LOCOS process. Following poly-Si deposition at 620 °C by LPCVD, they were *n*-doped under a 30 min $POCl_3$ processing at 950 °C. Therefore, we believe that MIS structures were subjected to postmetallization annealing processes at 950 °C for 30 min at the stage of $POCl_3$ processing.

Moreover, Raveh *et al.*[26] grew silicon dioxide (SiO_2) ~20 nm thick by means of thermal oxidation in a quartz furnace using dry oxygen at 900 °C for 15 min. In order to increase the concentration of Si–N bonds, they annealed their nitrided oxides for 15 min at temperatures between 200 and 700 °C under Ar at atmospheric pressures. They used Auger electron spectroscopy and atomic force microscopy to characterize the film morphology, composition and rms roughness of the layers, whereas grazing Fourier transform spectroscopy for determining the bonding feature at various depths. They showed that the *nitrogen concentration was more at the outer nitrided surface and decreased with respect to depth, indicating a diffusion profile for nitrogen into the oxide layer*. Therefore, they performed a two layer model for SE analysis depending on their variable measurement techniques, which is Si_3N_4 for the outer layer and SiO_2 for the inner layer *since nitrogen reactive species simply replace oxygen atoms in* SiO_2. Since our oxide films are 5 nm thick, it was not easy to obtain a homogeneous nitrided film through the film depth.

IV. RESULTS AND DISCUSSION

Temperature dependent current measurements with respect to a 5 nm thick reference SiO_2 and plasma nitrided SiO_xN_y oxides were studied to obtain the possible current mechanisms for certain electrical and temperature regimes. Current densities across the MOS structures were calculated for each specific *I-V* measurement. Figure 3 shows *I-V* plots at increased substrate temperatures in accumulation region of both oxides, additionally in the inversion region for reference oxide. Nevertheless, leakage current at inversion regime

TABLE I. Vertical furnace parameters used for the nitridation process on 5 nm thick SiO_2 oxide film. (SCCM denotes cubic centimeter per minute at STP.)

Duration (min)	Temperature (°C)	Pressure (mTorr)	N_2 (SCCM)	NH_3 (SCCM)	He (SCCM)	MW (W)	LF (W)	LF on (ms)	LF off (ms)
60	400	1200	1000	200	2100	2000	250	1	10

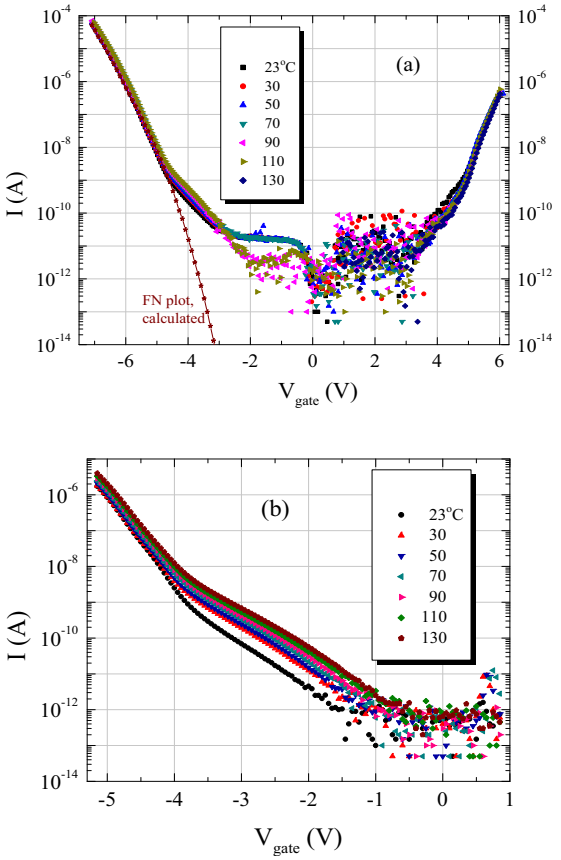

FIG. 3. (Color online) *I-V* plots for (a) 5 nm reference SiO_2 and (b) nitrided oxide film.

shows an opposite trend comparing the leakage current in accumulation regime. It seems that the leakage current decreases as the temperature increases. It is well known that minority carriers are effective in inversion regime. Since the number of minority carriers is not huge but much more limited, then their quantity changes are much applied physical conditions' dependent. Nevertheless, it is not clear why temperature increments' effect is in an opposite manner to that of accumulation regime.

It is highly important to know what kind of current conduction mechanism dominates under high applied *E*-field in the triangular barrier region of the oxide film to get information about the charge traps. One of the important mechanisms is FN tunneling current in which the current density is defined with:

$$J_{\mathrm{FN}} = AE_{ox}^2 \exp\left(-\frac{B}{E_{ox}}\right), \tag{1}$$

where J_{FN} is the current density of FN tunnel emission, E_{ox} is the *E*-field across the oxide, and *A* and *B* are defined as,

$$A = \frac{q^2 m}{8\pi h m^* \Phi_B}, \tag{2}$$

$$B = \frac{8\pi\sqrt{2m^*}}{3qh}(q\Phi_B)^{3/2}, \tag{3}$$

where Φ_B is the tunneling barrier height, m^* is the effective electron mass, h is the Planck constant, and q is the elec-

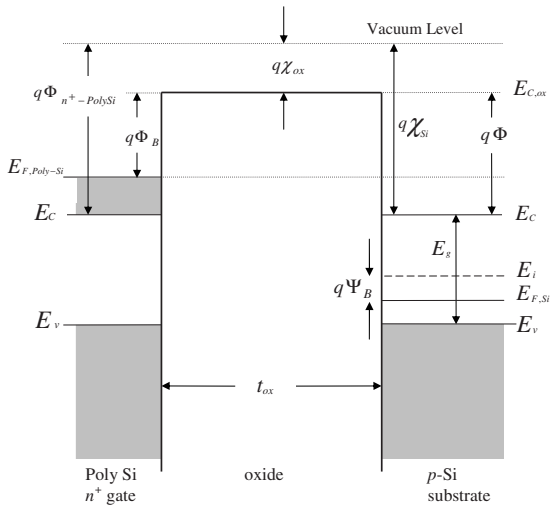

FIG. 4. Energy band diagram under flatband of MOS structure from n^+ poly-Si gate—oxide—*p* type Si substrate.

tron's charge.[10,27,28] E_{ox} is calculated in terms of applied gate voltage, V_g, and flatband voltage, V_{FB}, using Eq. (4). V_{FB} can be written using the energy band diagram of poly-Si gated MOS structure seen in Fig. 4. The electrical field through oxide and related potential equations are given in the following form:

$$E_{ox} = \frac{V_g - V_{FB} - \Psi_S - \dfrac{Q_{oxide}}{C_{acc}}}{t_{ox}}, \tag{4}$$

$$V_{FB} = \Phi_B - \Phi - \frac{E_g}{2} - \Psi_B, \tag{5}$$

$$\Psi_B = kT\,\mathrm{In}\left(\frac{N_A}{n_i(T)}\right), \tag{6}$$

where E_g, n_i, k, T, Ψ_B, Q_{oxide}, C_{acc} are, respectively, the Si bandgap energy, the intrinsic charge concentration, Boltzmann constant, absolute temperature, potential at the bulk semiconductor, effective oxide trapped charges in the nitride/SiO_2, and capacitance at accumulation.

The resistivity of *p*-Si substrate, 4–6 Ω cm, is used to obtain the doping concentration of Si substrate, N_A, ($\sim 2.5 \times 10^{15}/\mathrm{cm}^3$ at 300 K). E_g value of Si substrate depends also on the temperature changes as given in;

$$E_g(T) = E_g(0) - \frac{\alpha T^2}{T+\beta}, \tag{7}$$

where $E_g(0)$, α, β, T are used approximately as 1.166 eV, 4.73×10^{-4} eV/K, 636 K, and absolute temperature, respectively.[11,29] Intrinsic charge concentration values, n_i, for each absolute temperature corresponding to experimental ones were obtained from literature.[10]

The emitting electrode was formed as negatively charged degenerated poly-Si n^+ gate. The surface potential $\Psi_S(V_g)$ was calculated analytically by solving the one-dimensional Poisson's equation at each applied gate voltage.[10] An approximation to Fermi-Dirac distribution of the charge carri-

ers was used in the calculations. The silicon dioxide/silicon nitride gate stack was modeled using the respective dielectric constants ($k_{SiO_2}=3.9$, $k_{Si_3N_4}=7.5$) and layer thicknesses measured by ellipsometry. A homogeneous distribution of trapped charges evaluated from the RT *C-V* measurements was incorporated to adjust the gate voltages (Eq. (4)).

Flatband voltage V_{FB} and effective oxide charge Q_{oxide} values were obtained from the RT capacitance voltage measurements, C-V. Flatband voltages were -0.82 V for reference SiO_2 and -0.85 V for nitrided oxide. Oxide charges Q_{oxide} were approximately $-3.62\times10^{11}/cm^2$ for SiO_2 reference oxide and $-3.11\times10^{11}/cm^2$ for nitrided oxide. V_{FB} values for the specified increased sample temperatures of the current measurements were obtained from the experimentally measured RT V_{FB} value using the Eqs. (4)–(7).

Figure 2 shows the HRTEM picture taken from the cross sectional view of nitrided oxide. It is seen that a 2.5 nm thick nitrided oxide under the n^+ poly gate was followed by a 3.3 nm SiO_2 film on Si substrate. It is well known that the dielectric constant, k, of nitrided oxide lies somewhere between the value of SiO_2, 3.9, and that of nitride, Si_3N_4, film. EOT was drawn as 4.6 nm from the capacitance voltage measurements. Upon combining TEM thickness measurements with the EOT value [Eq. (8)], k value for nitrided oxide is obtained as 7.5 corresponding to thin nitride, Si_3N_4, film.

$$\mathrm{EOT} = d_{\mathrm{SiO_2}} + \left(\frac{3.9}{k_{\mathrm{SiON}}}\right) d_{\mathrm{SiON}}, \tag{8}$$

E_{ox_eff}–effective oxide fields were calculated using Eq. (4) with the EOT as 4.6 nm from *C-V* measurement of nitrided film.

When the natural logarithm of Eq. (1) is taken, the following FN equation is obtained;

$$\ln\left(\frac{J_{\mathrm{FN}}}{E_{ox}^2}\right) = \ln(A) - \frac{B}{E_{ox}}. \tag{9}$$

The plot of $\ln(J_{\mathrm{FN}}/E_{ox}^2)$ has a linear dependence on $(1/E_{ox})$ with;

$$\frac{q^2 m}{8\pi h m^* \Phi_B} = \exp(Intercept)$$

$$\text{and} \quad \frac{8\pi\sqrt{2m^*}}{3qh}(q\Phi_B)^{3/2} = |slope|. \tag{10}$$

Equation (10) is solved to obtain m^* and Φ_B for the reference SiO_2 and nitrided film;

$$\Phi_B = \frac{3}{4}\left(\frac{h_{3/2}}{q}\right)|slope|\sqrt{\frac{\exp(Intercept)}{\pi m}}, \tag{11}$$

$$m^* = \frac{q}{6\sqrt{\pi}}\left(\frac{q}{h}\right)^{5/2}\frac{1}{|slope|}\left(\frac{m}{\exp(Intercept)}\right)^{3/2}. \tag{12}$$

Figure 5 shows FN plots of $\ln(J_{\mathrm{FN}}/E_{ox}^2)$ with respect to $(1/E_{ox})$, i.e., E_{ox} for SiO_2 film from 23 to 110 °C and E_{nit} for nitrided oxide film for the temperature regime of 23 to 130 °C. From all these plots, it is clearly seen that there existed a high applied *E*-field regime corresponding to a linearly decaying function, and these regions can especially be given as E_{ox} becomes larger than 10.6 MV/cm for reference SiO_2 and 9.4 MV/cm for nitrided oxide, i.e., SiO_2 part of Si_3N_4/SiO_2 stack. The corresponding fitting equation is obtained in the form of $y=A+Bx$, where y defines $\ln(J_{\mathrm{FN}}/E_{ox}^2)$ and x defines $1/E_{ox}$. The fitting parameters of A and B for these two oxides, i.e., reference SiO_2 and nitrided oxide for each elevated temperatures are given in Table II.

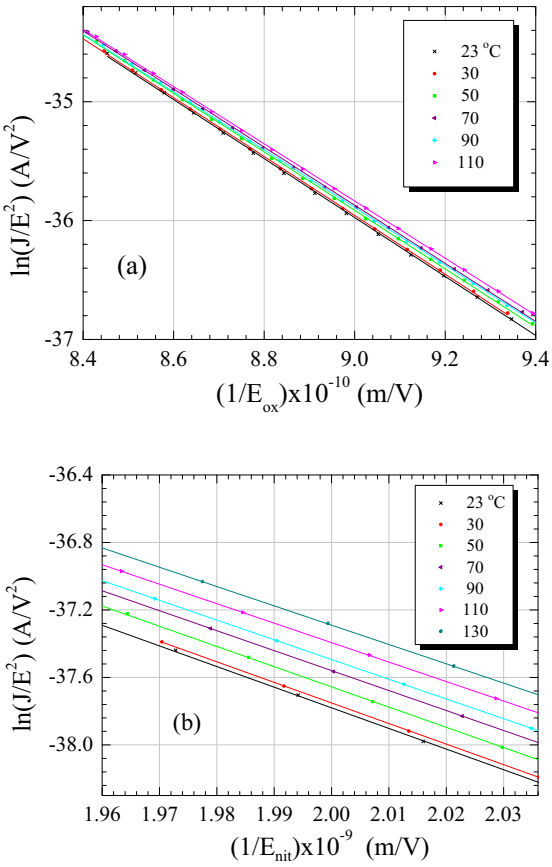

FIG. 5. (Color online) FN plots for (a) 5 nm reference SiO_2 and (b) nitrided oxide films.

Using these fitting parameters (Table II), barrier height Φ_B and electron effective mass m^* are calculated with respect to increased sample temperatures from 23 to 110 °C for SiO_2 and from 23 to 130 °C for nitrided oxide, i.e., SiO_xN_y thin films. Table III shows the tunneling barrier heights and effective electron masses for both type of oxides calculated from the FN fittings with respect to elevated temperature from 23 to 110 °C for SiO_2, and to 130 °C for nitrided oxide. It is clear that not only barrier height but also effective electron mass change extremely at the elevated substrate temperatures, even to extreme values for temperatures of higher than 70 °C.

It is also seen from the literature that the effective mass of electrons, m^*, is generally assumed to be changing between 0.36 and $0.5m_e$ for SiO_2 dielectric layer whereas the barrier height is between 3.1 and 3.2 eV. Nevertheless, some studies had shown a contradicting effect: If the effective mass is supposed to be $0.5m_e$, then barrier height is obtained around 2.9–3.1 eV,[30,31] whereas if barrier height is taken to be as 3.1 eV then effective mass was found as $0.37m_e$.[32]

TABLE II. Fitting parameters to natural logarithm function for each oxide layer at the specified elevated temperatures.

	Reference SiO_2				
		$y=A+Bx$			
Temp. (°C)	Adj. R^2	A	ΔA	B ($\times 10^{10}$)	ΔB ($\times 10^{7}$)
23	0.999 79	−13.653 48	0.080 58	−2.480 09	8.952 27
30	0.999 74	−13.678 45	0.094 54	−2.475 31	6.791 84
50	0.999 79	−13.772 68	0.081 07	−2.460 14	9.142 19
70	0.999 86	−13.878 86	0.062 00	−2.443 57	6.949 62
90	0.999 85	−14.033 57	0.055 80	−2.428 44	6.043 12
110	0.999 96	−14.186 37	0.027 40	−2.405 46	2.987 20
		Nitrided oxide			
23	0.999 88	−13.314 39	0.108 46	−1.223 29	5.435 04
30	0.999 94	−13.373 68	0.107 81	−1.218 88	5.381 95
50	0.999 93	−13.693 39	0.088 49	−1.198 13	4.430 27
70	0.999 99	−13.895 79	0.029 47	−1.183 19	1.472 63
90	1	−14.112 10	0.015 81	−1.169 09	0.789 55
110	0.999 99	−14.310 52	0.033 29	−1.154 16	1.667 65
130	0.999 98	−14.400 21	0.039 89	−1.144 50	2.005 26

Khairurrijal *et al.*[33] showed from their theoretical calculations that the effective mass of electrons in SiO_2 oxide film increases when the oxide thickness gets decreased, having a value between $0.3m_e$ and $0.9m_e$. Upon assuming constant electron effective mass at $0.5m_e$ in oxide film, Hadjadj *et al.*[22] added the effect of oxide thickness on electron affinity difference for 5, 7, and 12 nm thick oxides for the temperature ranging from 23 to 300 °C. They concluded that not only the temperature but also the oxide thickness had an effect on electron affinity difference and barrier height values under the used assumption of $0.5m_e$ for effective electron mass. Therefore, our results (Table III) show a good corre-

TABLE III. Barrier height (Φ_B) and effective mass (m^*) of charge carriers in terms of electronic charge's mass (m_e) are drawn from FN plots for a reference 5 nm thermally grown SiO_2 oxide and nitrided oxide films. It contains also barrier height values when effective mass is taken constant as $0.41m_e$ for SiO_2 and $0.50m_e$ for nitrided oxide.

	Reference SiO_2		
	Variable m^*		$m^*=0.41m_e$
Temperature (°C)	Φ_B (eV)	m^*/m_e	Φ_B (eV)
23	3.171 19 ∓ 0.139 22	0.413 36 ∓ 0.051 46	3.171 19 ∓ 0.007 63
30	3.125 80 ∓ 0.156 33	0.429 97 ∓ 0.062 15	3.167 11 ∓ 0.005 79
50	2.963 66 ∓ 0.131 15	0.498 30 ∓ 0.062 45	3.154 15 ∓ 0.007 81
70	2.791 50 ∓ 0.094 47	0.588 29 ∓ 0.056 38	3.139 97 ∓ 0.005 95
90	2.567 71 ∓ 0.078 03	0.746 58 ∓ 0.064 35	3.127 00 ∓ 0.005 19
110	2.356 33 ∓ 0.035 21	0.947 86 ∓ 0.040 14	3.107 24 ∓ 0.002 57
	Nitrided Oxide		
	Variable m^*		$m^*=0.50m_e$
Temperature (°C)	Φ_B (eV)	m^*/m_e	Φ_B (eV)
23	1.853 17 ∓ 0.108 73	0.503 93 ∓ 0.084 22	1.853 17 ∓ 0.005 06
30	1.792 55 ∓ 0.104 62	0.552 79 ∓ 0.091 86	1.848 71 ∓ 0.005 07
50	1.501 73 ∓ 0.072 00	0.908 43 ∓ 0.123 94	1.827 67 ∓ 0.004 15
70	1.340 26 ∓ 0.021 42	1.246 23 ∓ 0.056 64	1.812 44 ∓ 0.001 39
90	1.188 53 ∓ 0.010 20	1.744 68 ∓ 0.042 56	1.798 01 ∓ 0.000 46
110	1.062 54 ∓ 0.019 22	2.379 88 ∓ 0.122 29	1.782 68 ∓ 0.001 58
130	1.007 44 ∓ 0.021 86	2.745 56 ∓ 0.169 10	1.772 72 ∓ 0.001 91

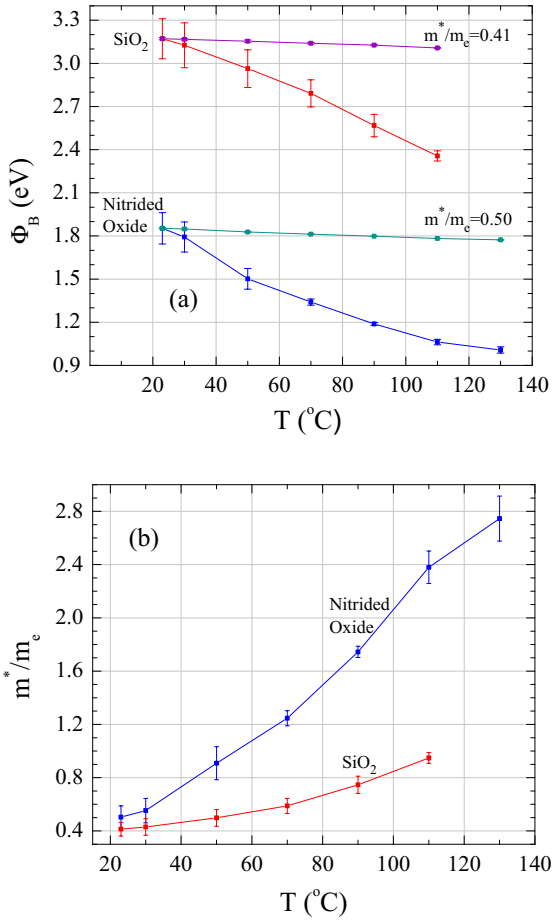

FIG. 6. (Color online) Barrier height ($\Phi_B \pm \Delta\Phi_B$) and effective electron mass ($m^* \pm \Delta m^*$) in reference SiO_2 and nitrided oxide.

spondence of tunneling barrier heights and effective electron masses at RT for SiO_2 oxide film comparable to the available literature data.

Figure 6 shows the tunneling barrier heights and effective electron masses with corresponding error bars calculated by means of absolute error propagation method for functions having two or more variables from the FN fits with respect to elevated temperatures ranging from RT to 110 °C for SiO_2 and to 130 °C for nitrided oxide film. It is clearly seen that tunneling depth levels are decreasing with respect to temperature increments, whereas effective mass behavior is detected with an opposite behavior to tunneling barrier heights as a result of temperature increments. It is observable that the increased temperature has similar effects on both oxides.

It is seen from Table III, in addition to Fig. 6 that the tunneling barrier heights decrease monotonically, while effective electron masses in oxide film increase in the same manner for both types of oxide films with respect to temperature increments. The values for barrier heights evaluated using a constant effective electron mass which is obtained for RT value as well as encountered in many studies as $0.41m_e$ in SiO_2 reference oxide and $0.50m_e$ in nitrided oxide, are also contained in Table III. However, not enough data for elevated substrate temperature is available in literature. Therefore, we can only compare our RT results to the literature data and detect that we obtained considerably good results.[15,22] In this work, we additionally added effect of high substrate temperatures on the barrier height and effective mass in a large range from RT to 110 °C for SiO_2 and 130 °C for nitrided oxide.

It is also seen from the literature that the effective mass of electrons is affected not only from the nitrogen content inside the oxide but also the thickness of the oxide film.[16,33,34] It is shown that there is a conflict, if the effective mass is taken as a constant when calculating the barrier height, or if the barrier height is taken as a constant when calculating the effective mass.[15] Some researchers additionally tried to formulize the effective mass, and/or barrier height in terms of nitrogen percentage content in the oxide film.[15,35]

From Fig. 6, it is seen that the effective electron mass in the nitrided oxide exceeds that of free electrons in vacuum at a substrate temperature of about 70 °C. Shashkin *et al.*[36] reported a sharp increase in the effective mass near the metal insulator transition. They explained this situation as two-dimensional electron systems becoming strongly correlated at sufficiently low electron densities, because the kinetic energy is overpowered by energy of electron–electron interactions. They declared that the value of the effective electron mass is strongly enhanced by more than a factor of 3 with decreasing the electron density. Therefore, the reason of effective electron mass increment as a result of elevated substrate temperature is better understood after the explanation of Shashkin *et al.*

V. CONCLUSION

This work contains the results of leakage current characteristics of plasma nitrided SiO_xN_y layers as well as of thermally grown 5 nm SiO_2 film by means of MIS structures of poly-Si electroded under the conditions of high applied *E*-field, i.e., FN regime, with respect to increased substrate temperatures. In contrast to literature work, we have obtained both effective mass and barrier heights for elevated temperatures from 23 to 110 °C for SiO_2 and to 130 °C for nitrided oxide without making any assumptions on either of them. We have shown that both parameters are affected from the temperature increments so that if we would assume one of them fixed and calculate the other one, then it would result in some incorrect physical properties. It was shown that tunneling barrier height was decreased and, oppositely, effective electron mass was increased at RT for the nitrided sample with respect to SiO_2 film. Additionally, effective electron mass and tunneling barrier heights at elevated substrate temperatures were calculated and compared to literature data.

From the available RT data in literature, we obtained good comparison for both oxides. Moreover, we have done the whole process not only at the RT but also for a temperature regime extending to 110 °C for SiO_2 and 130 °C for nitrided oxide. The results we obtained showed that there is a reduction in barrier height, while an increment in effective electron mass of both oxide films as a result of temperature increments. Therefore, these results can serve as a good technological evolution of a calculation method for current mechanism at high applied *E*-fields.

ACKNOWLEDGMENTS

This research was supported by the European Union Project of "Semiconductor Equipment Assessment for Nano-Electronic Technologies" (SEA-NET) with project Contract No. 027982. Authors thank Brigitte Amon for taking the HR-TEM picture.

[1]G. D. Wilk, R. M. Wallace, and J. M. Anthony, J. Appl. Phys. **89**, 5243 (2001).
[2]S. Ulucan, G. Aygun, L. Ozyuzer, M. Egilmez, and R. Turan, J. Optoelectron. Adv. Mater. **7**, 297 (2005).
[3]G. Aygun, E. Atanassova, A. Alacakir, L. Ozyuzer, and R. Turan, J. Phys. D: Appl. Phys. **37**, 1569 (2004).
[4]S. Buyukkose, S. Okur, and G. Aygun, J. Phys. D: Appl. Phys. **42**, 105302 (2009).
[5]M. L. Green, E. P. Gusev, R. Degraeve, and E. L. Garfunkel, J. Appl. Phys. **90**, 2057 (2001).
[6]G. Aygun, E. Atanassova, K. Kostov, and R. Turan, J. Non-Cryst. Solids **352**, 3134 (2006).
[7]G. Aygun and R. Turan, Thin Solid Films **517**, 994 (2008).
[8]G. Aygun and I. Yildiz, J. Appl. Phys. **106**, 014312 (2009).
[9]J. Dupuis, E. Fourmond, J. F. Lelièvre, D. Ballutaud, and M. Lemiti, Thin Solid Films **516**, 6954 (2008).
[10]S. M. Sze and K. K. Ng, *Physics of Semiconductor Devices* (Wiley, New York, 2007).
[11]B. El-Kareh, *Silicon Devices and Process Integration: Deep Submicron and Nano-Scale Technologies* (Springer, NY, USA, 2009).
[12]L. F. Mao and Z. O. Wang, Phys. Status Solidi A **204**, 784 (2007).
[13]J. F. Verwey, E. A. Amerasekera, and J. Bisschop, Rep. Prog. Phys. **53**, 1297 (1990).
[14]R. H. Fowler and L. W. Nordheim, Proc. R. Soc. London, Ser. A **119**, 173 (1928).
[15]C. Y. Ng, T. P. Chen, Y. Liu, C. Q. Sun, and S. Fung, J. Appl. Phys. **96**, 5912 (2004).
[16]R. Ludeke, E. Cartier, and A. Schenk, Appl. Phys. Lett. **75**, 1407 (1999).
[17]M. Fukuda, W. Mizubayashi, A. Kohno, S. Miyazaki, and M. Hirose, Jpn. J. Appl. Phys., Part 2 **37**, L1534 (1998).
[18]E. Nadimi, C. Golz, M. Trentzsch, L. Herrmann, K. Wieczorek, and C. Radehaus, IEEE Trans. Electron Devices **55**, 2462 (2008).
[19]M. Städele, F. Sacconi, A. D. Carlo, and P. Lugli, J. Appl. Phys. **93**, 2681 (2003).
[20]S. Horiguchi and H. Yoshino, J. Appl. Phys. **58**, 1597 (1985).
[21]L. F. Mao, Z. O. Wang, J. Y. Wang, and G. Y. Wang, Semicond. Sci. Technol. **20**, 1078 (2005).
[22]A. Hadjadj, G. Salace, and C. Petit, J. Appl. Phys. **89**, 7994 (2001).
[23]M. Costato and L. Reggina, Lett. Nuovo Cimento **3**, 239 (1970).
[24]L. F. Mao, Appl. Phys. Lett. **90**, 183511 (2007).
[25]M.-H. Cho, K. B. Chung, Y. K. Kim, D. C. Kim, J.-H. Heo, B. Y. Koo, Y. K. Shin, U. I. Chung, J. T. Moon, and D.-H. Ko, Electrochem. Solid-State Lett. **9**, F27 (2006).
[26]A. Raveh, J. Brewer, and E. A. Irene, J. Vac. Sci. Technol. A **19**, 17 (2001).
[27]M. Lenzlinger and E. H. Snow, J. Appl. Phys. **40**, 278 (1969).
[28]M.-T. Wang, T.-H. Wang, B. Yi-Yi Cheng, and J. Ya-min Lee, J. Electrochem. Soc. **153**, F8 (2006).
[29]G. Salace, A. Hadjadj, C. Petit, and M. Jourdain, J. Appl. Phys. **85**, 7768 (1999).
[30]P. Olivo, J. Sune, and B. Ricco, IEEE Electron Device Lett. **12**, 620 (1991).
[31]H. Fujioka, C. Wann, D. Park, and C. Hu, *Surface/Interface and Stress Effects in Electronic Materials Nanostructures*, MRS Symposia Proceedings No. 405, Boston, MA, 27 November—1 December 1995 (Materials Research Society, Pittsburg, PA, 1996), p. 333.
[32]T. C. Yang, P. Sachdev, and K. C. Saraswat, IEEE Trans. Electron Devices **46**, 1457 (1999).
[33]Khairurrijal, W. Mizubayashi, S. Miyazaki, and M. Hirose, J. Appl. Phys. **87**, 3000 (2000), and references therein.
[34]C. Y. Ng, T. P. Chen, and C. H. Ang, Smart Mater. Struct. **15**, S39 (2006).
[35]S. S. Tan, T. P. Chen, and C. H. Ang, J. Appl. Phys. **93**, 3114 (2003).
[36]A. A. Shashkin, M. Rahimi, S. Anissimova, S. V. Kravchenko, V. T. Dolgopolov, and T. M. Klapwijk, Physica E **22**, 224 (2004).